Conformational and Structural Changes of Choline Oxidase from *Alcaligenes* Species by Changing pH Values

A. Hekmat, A. A. Saboury,[*] A. Divsalar, and M. Khanmohammadi[†]

Institute of Biochemistry and Biophysics, University of Tehran, P.O. Box 13145-1384, Tehran, Iran. [*]E-mail: saboury@ut.ac.ir
[†]Department of Chemistry, Faculty of Science, University of Qazvin, Qazvin, Iran
Received June 9, 2008

Results of intrinsic and extrinsic fluorescence studies on choline oxidase revealed that the enzyme at high alkaline pH values has more accessible hydrophobic patches relative to acidic pH. Fluorescence quenching studies with acrylamide confirm these changes. The quenching constants were also determined at different pH(s) by using the Stern-Volmer equation. CD studies showed that at higher pH a transition from α-helix to β-structure was appeared while at lower pH the content of α-helix structure was increased. Furthermore, analysis of the spectral data using chemometric method gave evidence for existence of intermediate components at very high pH(s). Results of thermal denaturation evaluated that the enzyme has the most instability at higher pH(s). Altogether low and high pH values caused significant alteration on secondary and tertiary structures of choline oxidase via inducing of an intermediate.

Key Words : Choline oxidase, pH, Chemometry analyses, Fluorescence quenching, Circular dichroism

Introduction

It is well known that hydrophobic interactions are important determinants of protein structure, which most hydrophobic group of amino acid residues are found in the interior of proteins. When hydrophobic groups are found on the surface of proteins, they are often thought to have functional roles as interaction sites for small molecules, other proteins, and membranes. Hydrophobic regions in proteins have thus been the objects of numerous studies. These studies include detection of hydrophobic sites by binding to active sites of enzymes,[1,2] pH and ligand-induced conformational changes.[3-5] Normally, enzymes are only active over a limited range of pH and in most cases, a definite optimum pH is observed. The fall of activity on either side of the optimum may be related to the effect of pH on the stability of the enzyme, which may be irreversibly destroyed on one or both sides of the optimum pH.[6] From a fundamental standpoint, changes in pH can bring about changes in enzyme conformation, which in turn can affect the enzyme interaction with the substrate, and its activity. In fact, protein unfolding and denaturation at low and high pH is quite a general phenomenon. This reasons motivated us to study the effect of pH on choline oxidase (ChOx, E.C. 1.1.3.17) conformation from *Alcaligenes* species.

Bernheim first demonstrated the presence of choline oxidase in animal tissues.[7] Afterward a great deal of work has been carried out to study this enzyme in details.[8,9] Choline oxidase was first isolated from rat liver in 1938.[10] At that time, it was publicized that choline oxidase system was composed of choline dehydrogenase, cytochrome c, and cytochrome oxidase.[10] In 1977, Ikuta reported the purification of the enzyme from soil bacterium *Arthrobacter globiformis*.[11] In addition, the enzyme was purified from other microorganisms, such as *Cylindrocarpon didymium*[12]

and *Alcaligenes* species.[13,14] Although the amino acid sequence of choline oxidase from *Arthrobacter globiformis* has been determined and reported but, such information about the choline oxidase from *Alcaligenes* species has not been reported.

Choline oxidase, a FAD-containing enzyme, catalyzes the oxidation of choline to glycine-betaine (*N,N,N*-trimethylglycine) with betaine aldehyde as an intermediate and molecular oxygen as primary electron acceptor.[15] The molecular weight of the enzyme was estimated to be 66 kDa for a monomer.[14] The prosthetic group of the enzyme from *Alcaligenes* species was identified as 8a-[N (3)-histidyl]-FAD and the partial sequence of amino acids in the flavin peptide reported as: Asp-Asn-Pro-Asn-His-(FAD)-Ser-Arg.[13] Absorption and circular dichroism (CD) spectra of ChOx suggest that the environment surrounding and spatial orientation of the flavin have a major role in the enzyme activity.[16] In addition, the pH and kinetic isotope effect studies on ChOx has been shown that a catalytic base with a pK_a value of 7.4 is essential for the enzyme-catalyzed a oxidation of choline to glycine aldehyde and then betaine[15,17] and this characteristic seems to be compatible with histidine.[18]

The investigation on choline oxidase is of interest to scientists for some different reasons. The mechanism of the carbon–hydrogen bond cleavage in the choline by ChOx is important because of the high energetic barrier associated with this process.[15] This reaction also is of considerable importance for medical and biotechnological reasons; due to the accumulation of glycine betaine (GB) has been observed in a number of human pathogenic bacteria and the cytoplasm of many plants in response to hyperosmotic and temperature stresses, hence resulting in the prevention of dehydration and cell death. GB also protects the transcriptional and translational machinery by decreasing the melting temper-

ature *in vitro* of double-stranded DNA. This seems to suggest that GB behaves like chaperonin.[19-30] In addition, the development of biosensors for detection of choline, choline derivatives and organophosphorous compounds in biological[31] and environmental samples (include air, soil and water),[32,33] render this enzyme of clinical and industrial interest.

Despite the large amount of work, the mechanism of pH-dependent structural changes on choline oxidase is not available yet. This reasons inspired us to study the effect of various pH conditions on the conformation of choline oxidase. At first, we employed Nile red as the neutral fluorescence probe to monitor of pH-induced changes in the surface hydrophobicity of choline oxidase. In addition, we used the Trp residues in choline oxidase as intrinsic probes and measured changes in their fluorescence as a function of pH. These changes can, in principle, produce changes in the position or orientation of the tryptophan residues, altering their exposure to solvent and leading to an alternation in the quantum yield.[34] Subsequently, experiments on quenching of choline oxidase fluorescence by acrylamide as a quencher were performed to further characterize of pH on choline oxidase.

To complete the investigation of the conformational changes in the secondary structure of choline oxidase at different pH values, we also carried out Far-UV CD (Circular Dichroism) experiments. Finally, we utilized UV-vis experiments of choline oxidase at different pH values. UV-vis absorbance spectroscopy is the simplest spectroscopic methods to investigate the chemical or physical properties of proteins but spectral band overlapping is a major problem concerned with this method. However, by the use of chemometrics methods one can utilize the entire range of spectral data and thereby analyze the system under study using existing chemometrics algorithms.[35] Multivariate curve resolutions (MCR) are part of a family of chemometrics methods that deal with complex chemical equilibria through an evolutionary process.[36,37] For these reasons, we employed multivariate curve resolution method to study the effect of pH on the structure of choline oxidase.

It is important to mention that this is the first attempt to study the structural changes of choline oxidase from *Alcaligenes* species induced by low and high pH at different temperatures of 27 and 37 °C. All of the Information obtained from this study will be helpful to the understanding of the effects of pH on the choline oxidase from *Alcaligenes* species conformation.

Materials and Methods

Materials. Choline oxidase (E.C. 1.1.3.17 from *Alcaligenes* species) and Nile red (9-diethylamino-5H-benzo phenoxazine-5-one) were supplied by Sigma (St. Louis, MO, USA). Tris-(hydroxyl-methyl)-methylen were from BDH Chemicals Ltd. and Aldrich (St. Louis, MO, USA), respectively. Acrylamide was purchased from Merck (Darmstat, Germany).

Methods

UV-Vis Measurements: Choline oxidase (2 μM) was exposed in 100 mM Tris-HCl in the pH range 3-11. Afterward the UV-vis spectra of the protein in the range of 200-350 nm were obtained with UV-spectrophotometer Shimadzu, model UV-3100 at 37 °C. The system was first baselined with buffer solutions and then protein spectra at various pH values were obtained.

Enzyme Assay: Initial velocity of choline oxidase catalyzed reaction was determined using the procedure described by Sigma-Aldrich in details[38] in a Shimadzu, model UV-3100 spectrophotometer, equipped with a temperature control system. A stock solution of choline oxidase (96.8 μM) was prepared in 10 mM Tris-HCl at different pH(s) containing 134 mM KCl and 2 mM EDTA. Choline oxidase was assayed in a mixture containing 1 mL of 100 mM Tris-HCl (pH 8.0), 5 units/mg HRP, 50 mM of 4-aminoantipyrine and 150 mM of choline chloride as a substrate at 27 and 37 °C. The reaction was started by the addition of 20 μL of ChOx in the temperature-controlled (27 and 37 °C) cuvette compartment. The enzyme reaction was monitored spectrophotometrically at 500 nm by the production of quinonimine dye. The initial velocity of enzyme was calculated using an absorption coefficient, $\varepsilon = 12,000$ M^{-1} cm^{-1} and one unit of enzymatic initial velocity is given as μmol/min.

Fluorescence Measurements: Fluorescence emission spectra were measured in a Hitachi model MPF-4 fluorescence spectrophotometer equipped with temperature controller Protherms bath model NTB-211. The excitation and emission wavelengths were 530 and 550 nm for Nile red and 285 and 300 nm for Trp fluorescence. In all cases, 5 and 10 nm excitation and emission slits were used. At high concentrations of the probe or a quencher, fluorescence was corrected for inner-filter effect.

To study the effect of pH, samples contained 30 μM Nile red and 2 μM choline oxidase in 100 mM Tris-HCl in the pH range 3-11 were prepared. The Nile red spectra were corrected for probe's own response to pH in the absent of protein, because Nile red fluorescence is pH-sensitive. The fluorescence spectrum for each sample was recorded after 30 min incubation at 27 and 37 °C.

Quenching studies were performed by adding the quencher to both sample and the blank cell at 27 and 37 °C. Protein concentration was 2 μM at different pHs (pH 4, 6, 8 and 10) for 30 min at 27 and 37 °C. Quenching titrations with acrylamide were performed with sequentially added aliquots of quencher stock solution (8 M) to the samples at different pH values. The excitation and emission wavelength was set at 285 and 300 nm. Fluorescence intensity was corrected for background, adjusted for dilution by titration and corrected for inner filter effects. The inner filter effect due to acrylamide absorption was corrected according to the following equation:[39]

$$F_{corr} = F \cdot 10^{\frac{A}{2}} \qquad (1)$$

Here, F_{corr} and F are the corrected and observed fluore-

scence intensities, respectively, and A is the absorbance in the 1-cm cell at 285 nm. The fluorescence quenching data in the presence of acrylamide were analyzed by fitting to Stern-Volmer equation:[40]

$$\frac{F_0}{F} = 1 + K_{SV}[Q] \tag{2}$$

Where F_0 is the fluorescence in the absent of the quencher, F is the fluorescence in presence of the quencher at the concentration $[Q]$, and K_{SV} is the quenching constant.

Circular Dichroism (CD) Measurements: The secondary structure estimation of protein was studied using the Aviv circular dichroism (CD) spectrometer, Model 215. The CD spectrum of choline oxidase at different pH values was recorded from 200 to 250 nm Using a quartz cell, 0.1 cm pathlength, with a resolution of 0.2 nm, scan speed of 20 nm min^{-1}, time constant of 2.0 s, 10 nm band width and sensitivity of 20 m°. The fixed concentrations of ChOx in 100 mM Tris-HCl buffer, at different pH, at 27 and 37 °C were kept at 41.4 μM. All spectra were corrected by subtracting the proper baseline.

Temperature dependences of ellipticity at 222 nm were recorded under the same condition as Far-UV-CD in the temperature range of 25-100 °C with the constant heating rate of 1 K min^{-1}.

Chemometric Analysis: For each system under study, the absorbance data were digitized in the 0.5 nm intervals and gathered in a (m × n) data matrix **D** where m and n are the number of titration steps and number of wavelength, respectively. Thus, each row of matrix **D** was a digitized spectrum in an individual titration step (*i.e.* different pH values). This data matrix was then subjected to factor analysis to evaluate the number of components. For this purpose, the data matrix was decomposed to row and column matrices by singular value decomposition (SVD) as:

$$D = TP \tag{3}$$

Where **T** and **P** contain the orthogonal eigenvectors spanning the row and column spaces of the original data set, respectively. Some different methods, such as real error (RE), imbedded error (IM), chi value (χ), and indicator function are available for determining the number of factors.[41] The MCR-ALS subroutine written by Tauler was used to resolve the components of pure spectra and their corresponding pH profiles. The ALS program was downloaded from the site: http://www.ub.es/gesq/mcr/ mcr.htm

Here, the MCR-ALS analysis decomposes the data matrix **D** into a matrix **C** of the pure pH profile, and a matrix **S** of pure spectral profile, related to different species of iodine in the solvent system:

$$D = CS + E \tag{4}$$

In an iterative procedure, **C** and **S** are calculated so that the **CS** product constructs the original data matrix **D** with the optimal fit (*i.e.*, at a minimal residual error, **E**) based on the two following matrix equations:

$$C = DS^+ \tag{5}$$

$$S = C^+D \tag{6}$$

The superscript '+' denotes the pseudo-inverse of a matrix. An initial guess of the pH profile or pure spectra is needed to start the ALS optimization. Here, the evolving-factor analysis (EFA) was used to obtain the first estimate of the pH profiles of the components. In each iterative cycle of optimization, some constraints were applied. The non-negativity, unimodality, and closure constraints were used for pH of the profiles, and non- negativity was applied to the spectral profiles. For more information about MCR-ALS, one may refer to the papers by Diaz-Cruz *et al.*[36]

Results

The pH-dependent Conformation Changes in Choline Oxidase. Several studies have identified surface hydrophobic sites on proteins by observing the fluorescence enhancement of polarity sensitive dyes like ANS on addition to the proteins. While ANS is negatively charged probe, electrostatic interactions may play a role in the binding of the probe to the protein. Furthermore, it has been demonstrated that the probe itself can induce conformation changes in proteins.[42] In order to exclude these possibilities, we used another polarity-sensitive probe, neutral Nile red. Many reports in the literature confirm that the probes' quantum yields depend strongly on the polarity of their environment:
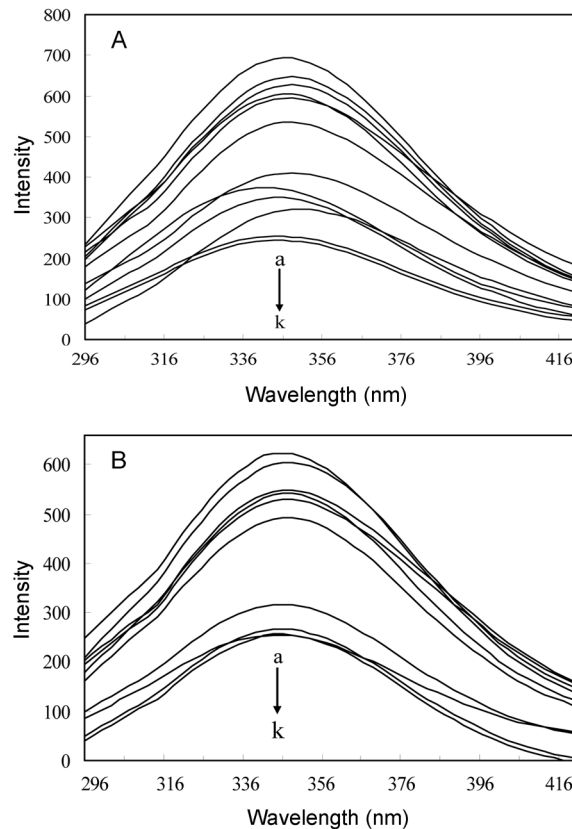

Figure 1. The intrinsic fluorescence emission spectra of choline oxidase (2 μM) in the presence of Nile red (30 μM) and in the pH 11(a), 10 (b), 9(c), 8.5(d), 8(e), 7.5(f), 7(g), 6 (h), 5 (i), 4 (j) and 3 (k) at 27 (A) and 37 °C (B).
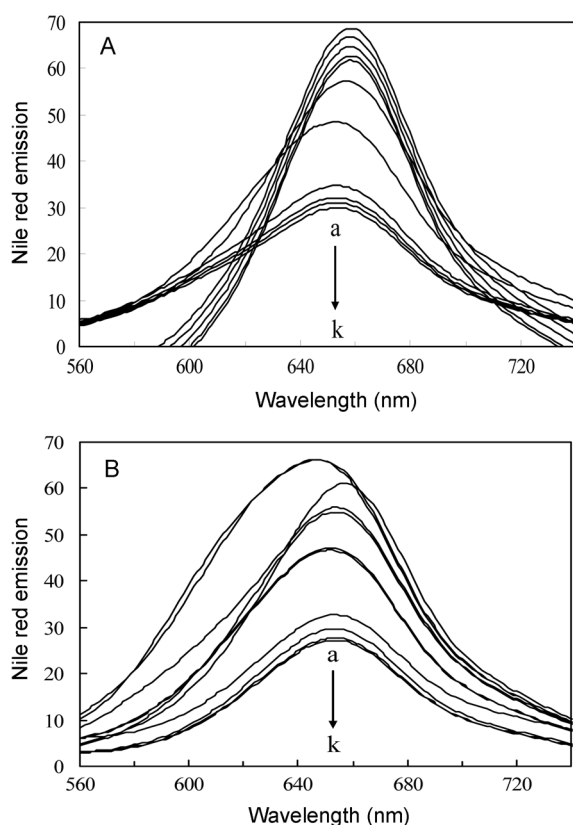
Figure 2. The fluorescence emission spectra of Nile red (30 μM) after exposing choline oxidase at various ranges of pH at 27 (A) and 37 °C (B). a, b, c, d, e, f, g, h, i, j and k represent the spectra at pH 11, 10, 9, 8.5, 8, 7.5, 7, 6, 5, 4 and 3.

Figure 3. (A) pH dependence of the fluorescence intensity of Nile red in the presence of choline oxidase at 27 (♦) and 37 (■) °C. Concentration of the dye was 30 μM (Nile red) and that of the enzyme was 2 μM. (B) pH dependence of Trp fluorescence in presence of Nile red at 27 (♦) and 37 (■) °C.

their fluorescence increases upon binding to hydrophobic sites on the protein.[43,44] Figure 1 shows the intrinsic fluorescence emission spectra of choline oxidase in the presence of Nile red and in the pH range between 3 and 11 at 27 and 37 °C when the data were corrected for the probe's own response to pH in the absence of protein. Figure 2 illustrates the fluorescence emission spectra of Nile red after exposing choline oxidase at various ranges of pH at 27 and 37 °C. These figures demonstrate an increase in the fluorescence by increasing pH values, which approaches a maximum at pH 11.

Figure 3 shows plots of the maximum emission intensity at 341 and 610 nm at 27 and 37 °C corresponding to spectra a-k in Figures 1 and 2. As shown in Figure 3, in the pH range between 3 and 5 the quantum yield remained at low levels but at higher alkaline pH values the quantum yield of the probe tripled. The observed increase the fluorescence intensity is due to the increased binding of Nile red, which is the result of exposure of buried hydrophobic amino acid residues on the protein surface. According to Figure 3, it is interesting to point out that at pH 8 the protein has more accessible hydrophobic patch than acidic pH(s). The apparent pK_a (the mid-point of each plots of Figure 3) of this conformation change in choline oxidase is 6.5 at both 27 and 37 °C.

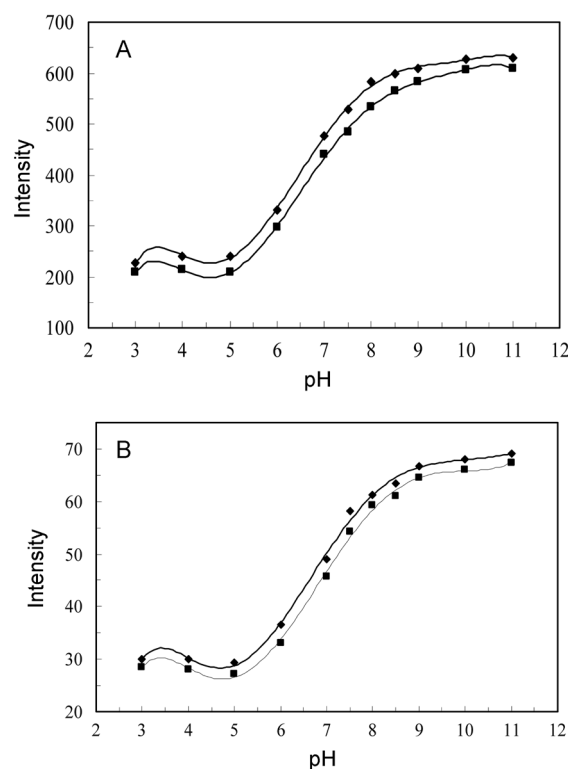Intrinsic Trp fluorescence was also used to monitor pH-

induced changes in the protein conformation after incubation for 30 min at 27 and 37 °C (Figure 4). A decrease in pH from 6 to 3 caused a decrease of Trp fluorescence intensity but when pH was higher than 9 the fluorescence intensity decreased. Furthermore, a tryptophan emission maximum of the enzyme was 4 nm red-shifted, reaching 344 nm at pH 10 (Figure 4). This indicates that at very high alkaline pH values, the tryptophan residues are gradually expose to more hydrophilic environment.

Fluorescence Quenching. Acrylamide quenching has been used to provide insights into conformational changes of proteins by probing the solvent accessibility of fluorescence moieties.[45,46] Quenching titration were performed with sequentially added aliquots of acrylamide solutions to choline oxidase samples at different pH values at 27 and 37 °C. Figure 5 shows Stern-Volmer plots for the tryptophan fluorescence quenching of choline oxidase by acrylamide at various pH values. Each line was obtained by linear fitting with the coefficient above 0.99. Stern-Volmer constants (K_{SV}) can be obtained from the slope of each linear relationship by using Stern-Volmer equation (Eq. 2) and are presented in Table 1. According to Table 1 and Figure 5, the significant increase in the solvent accessibility of tryptophan residues was observed at pH 10, which is consistent with the data from the intrinsic and Nile red fluorescence experiments furthermore, at pH 8 the quenching was lower than other pHs of this experiment. More importantly, when the
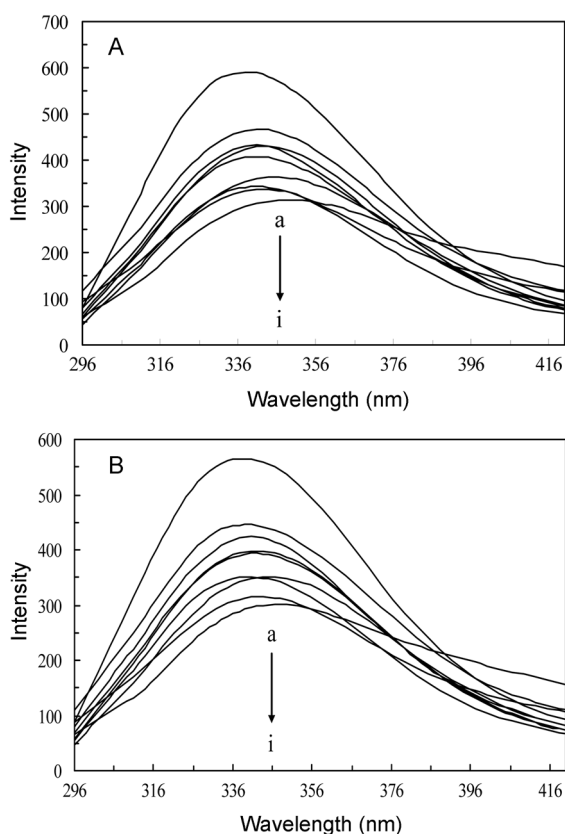
Figure 4. Intrinsic Trp fluorescence of choline oxidase after incubation for 30 min at pH 9 (a), 7 (b), 5 (c), 4 (d), 3 (e), 6 (f), 8 (g), 10 (h) and 11 (i) at 27 (A) and 37 °C (B).

temperature was increased from 27 to 37 °C, the K_{SV} of each pH doubled. On the other hand, fluorescence quenching of choline oxidase is pure collisional quenching.

Circular Dichroism Studies. Far-UV CD spectra (190-260) are used for determination of the secondary structure of a protein. The peptide bond is the principal absorbing group and studies in this region can give information on the secondary structure.[47,48] In order to consider the effect of different pH values and temperature on the conformational changes of choline oxidase, Far-UV CD technique has used and the spectra were reported in Figure 6 for the enzyme that incubated at different pH values.

The spectra of enzyme at pH 8 at both 27 and 37 °C show significant negative bandwidth double minima at 208 and 222 nm, which are the characteristic of α-helix (Figure 6d). Tables 2 and 3 indicate the content of the secondary structures of choline oxidase under various pH values at 27 and 37 °C. Interestingly, high alkaline pHs (pH 9 and 10) affected on the secondary structure of choline oxidase and a transition from α-helix to β-structure was appeared (Figure 6a, b and Tables 2 and 3). It should be point out that at very acidic pH values (pH 3 and 4) the content of α-helical structure significantly increased (Figure 6e, f and Tables 2 and 3). By comparing the content of α-helical structure at very acidic pH and pH 8, we can conclude that the enzyme at pH 8 is more flexible than very acidic pH. Figure 6 confirms that various pH values caused the changes in the
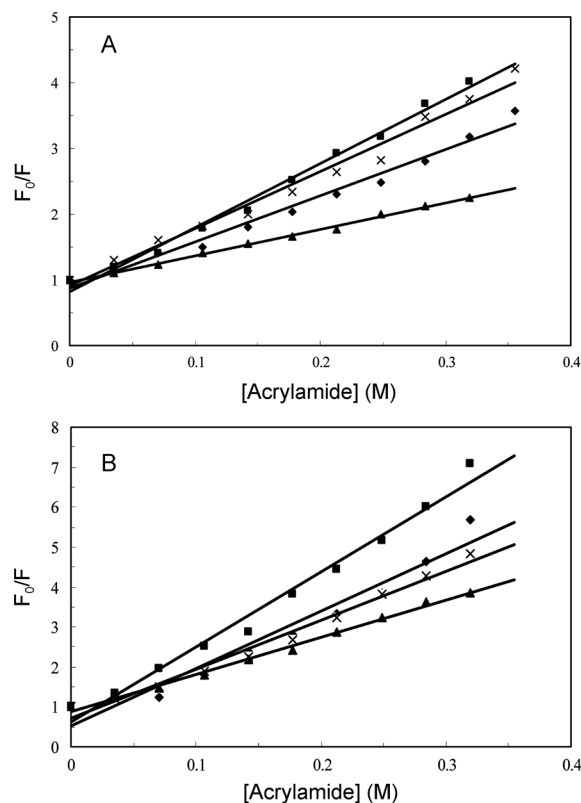

Figure 5. The Stern-Volmer curves for Acrylamide quenching of choline oxidase under various pH conditions: pH 4 ($\times$), 6 ($\blacklozenge$), 8 ($\blacktriangle$) and 10 ($\blacksquare$) at 27 °C (A) and 37 °C (B).

Table 1. The Stern-Volmer constants of the choline oxidase fluorescence quenching by acrylamide at various pH values and at 27 and 37 °C

pH	K_{SV} (M^{-1}) at 27 °C	K_{SV} (M^{-1}) at 37 °C
4	0.13	0.22
6	0.15	0.25
8	0.07	0.16
10	0.17	0.33

secondary structure of the choline oxidase. This elucidates that these changes consequently prevent the access of the substrate (choline chloride) to the enzyme active site. Figure 6 also indicates that with a rise of 10 °C in temperature, the overall shape of the spectra do not change significantly.

Thermal Denaturation. Thermal denaturation profiles of choline oxidase obtained from thermal scanning, under different pH values are depicted in Figure 7A. Each profile is a sigmoidal curve, thus this process is described as a single denaturant-dependent step according to the two-step theory.[49] The determination of standard Gibbs free energy of denaturation ($\Delta G°$), as a criterion of conformational stability of a globular protein, is based on two-state theory as follows:

$$\text{Native (N)} \Leftrightarrow \text{Denatured (D)} \qquad (7)$$

By assuming two-state mechanism for protein denaturation, one can determine the process by monitoring changes in the absorbance or elipticity and hence calculate the denatured
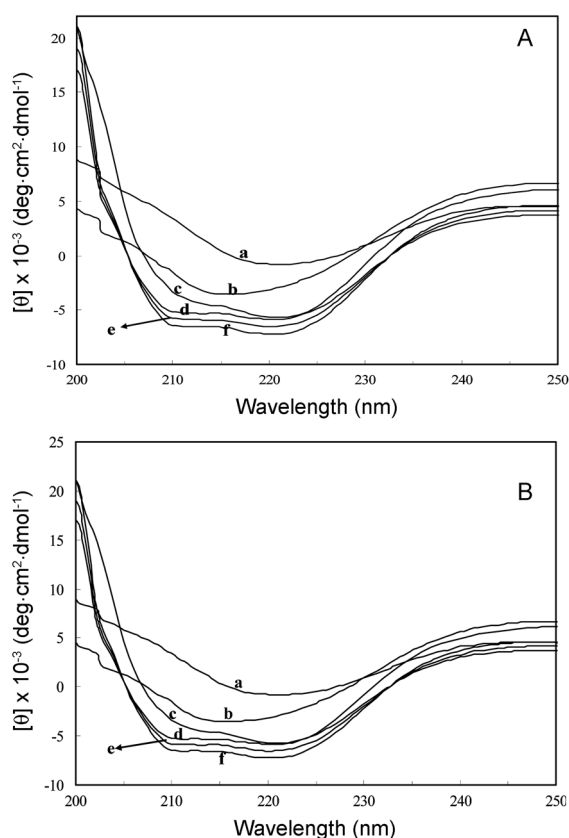
Figure 6. The pH-dependent structural changes of choline oxidase (41.4 μM) analyzed by Far-UV circular dichroism spectra after incubation at pH 10 (a), 9 (b), 6 (c), 8 (d), 4 (e) and 3 (f) at 27 °C (A) and 37 °C (B).

Table 2. Content of the secondary structure of choline oxidase at different pH values at 27 °C

pH	α-Helix (%)	β-Sheet (%)	Random coil (%)
3	82.1	9.2	8.7
4	77.8	11	11.2
6	67.4	13.2	19.4
8	78	9	13
9	32	35	33
10	9.6	44	46.4

Table 3. Content of the secondary structure of choline oxidase at different pH values at 37 °C

pH	α-Helix (%)	β-Sheet (%)	Random coil (%)
3	81.5	9.4	9.1
4	77.3	9.3	13.4
6	67.8	13.1	19.1
8	77	8	15
9	33	32	35
10	9.2	45	45.8

fraction of protein (F_d) as well as determination of the equilibrium constant (K).

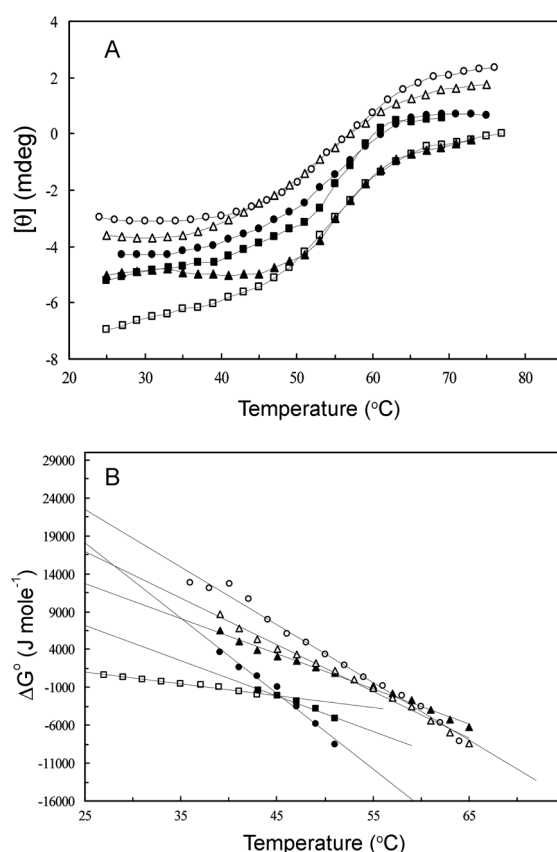$$F_d = \frac{Y_N - Y_{obs}}{Y_N - Y_D} \qquad (8)$$

Figure 7. (A) Thermal denaturation curves for choline oxidase (41.4 mM) obtained from molar ellipticity [θ] at 222 at pH 3 (▲), 4 (△), 6 (●), 8 (○), 9 (■) and 10 (□). (B) Linear extrapolation method for calculation of free energy and T_m of choline oxidase at pH 3 (▲), 4 (△), 6 (●), 8 (○), 9 (■) and 10 (□).

$$K = \frac{F_d}{1 - F_d} = \frac{Y_N - Y_{obs}}{Y_{obs} - Y_D} \qquad (9)$$

Where Y_{obs} is the observed variable parameter (*e.g.* absorbance or elipticity), Y_N and Y_D are the values of Y characteristics of a fully native and denatured conformation, respectively. The standard Gibbs free energy change (ΔG°) for protein denaturation is given by the following equation:

$$\Delta G^{o} = -RT \ln K \qquad (10)$$

Where R is the universal gas constant and T is the absolute temperature. ΔG^{o}_{25} (the standard Gibbs free energy of protein denaturation at 25 °C) is the most valuable criterions of protein conformational stability in the process of thermal denaturation. This criterion is obtained from the least-square analysis illustrated in Figure 7B. ΔG^{o}_{25} values are obtained from Y-intercepts of these replots (Figure 7B). In thermal denaturation, protein melting point (T_m) is a temperature that need for protein receiving to half of its two-state transition. Magnitudes of ΔG^{o}_{25} and T_m determined from replots, are summarized in Table 4. ΔG^{o}_{25} is estimated to be the highest for choline oxidase that incubated at pH 8 (22.5 kJ/mol), while in the case of high pH values ΔG^{o}_{25} is obtained 1 kJ/mol. This result revealed that the most instability occurred at higher pH values. Comparison of these magnitudes reveals
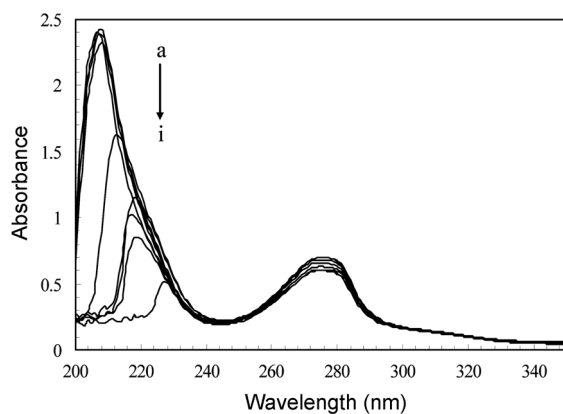
Table 4. Thermodynamic parameters of thermal stability of choline oxidase at different pH values

pH	T_m (°C)	ΔG^o_{25} (kJ mol^{-1})
3	52	13
4	53	17
6	56	18.5
8	58	22.5
9	50	7
10	49	1

that the nature of enzyme differs from in the different pH values.

Chemometric Analysis. Figure 8 shows plots of UV-vis absorption of choline oxidase at various pH(s). It is seen in this figure that at 280 nm region with changing pH, no significant and orderly changes in absorption took place whereas at 230 nm which is refer to peptide bond with increasing pH, absorption decreased. In addition, a red shift was observed in a maximum emission wavelength (λ_{max}) at higher alkaline pH(s). The UV-vis spectra obtained in this section were the crude data for chemometric analysis to determine the number of total compounds present in the solution. Since our previous data showed that choline oxidase has maximum efficiency at pH 8 and be in its native form, thus by assuming 100% efficiency for pH 8, we determined efficiency of other pH values with MCR-ALS analysis. Table 5 indicates the percent of performances at different pH values. It is seen that at acidic pH values the percent of performances are constant consequently there is only one species at this range of pH values. On the other hand, at very alkaline pH(s) these values are altered and two significant species were estimated. In addition, at pH 7 and 9 significant intermediates were observed. This result is consistent with the data from CD experiments and confirms the existence of intermediate components at very high pH(s).

Activity Studies. The effect of pH on the activity of choline oxidase can be determined by carrying out a series of velocity measurements at different pH(s). As shown in Figure 9 the enzyme has the optimal activity at pH 8 at both
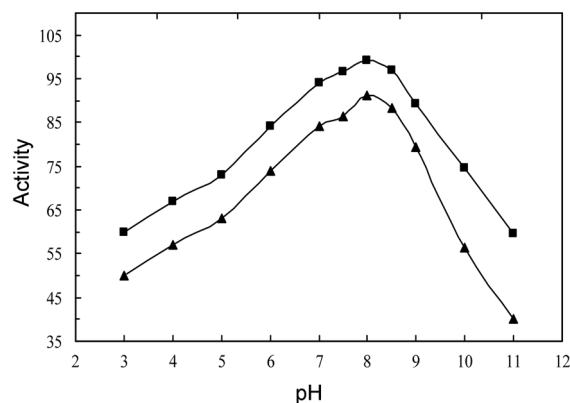
Table 5. The percent of Performance of choline oxidase at different pH using chemometric analysis

pH	Performance (%)
3	73.88
4	72.55
5	74.37
6	73.17
7	83.33
8	100
9	82.24
10	74.39
11	63.23

temperatures of 27 and 37 °C. The main inactivation of choline oxidase, as seen in Figure 9, took place in the pH ranges 3-6 and 9-11, which is related to changes in the structure of the enzyme. Figure 9 also revealed a more rapid inactivation of alkaline than of acidic pH values at both temperatures. Altogether, we can conclude that low and high pH values caused significant alteration on secondary and tertiary structures of choline oxidase, which can cause fall in the activity of the enzyme.

Discussion and Conclusion

In the present study, fluorescence, UV-vis spectroscopy and CD techniques have been used to monitor the changes of conformation of choline oxidase induced by pH. The interaction of an extrinsic probe (Nile red) with an enzyme (choline oxidase) in solution was investigated using fluorescence techniques. Nile red fluorescence is very environmentally sensitive and the presence of domains of differing polarity within the enzyme was ascertained by the decomposition of the Nile red emission spectrum. Thus we discovered that at both 27 and 37 °C with increasing pH, increased its affinity toward the hydrophobic patch of enzyme. The apparent pK_a of this conformation change in choline oxidase is 6.5 at both 27 and 37 °C. Subsequently pH-induced changes were observed in intrinsic fluorescence intensity of the Trp residues in choline oxidase: in the

Figure 8. UV-vis spectra of choline oxidase (2 μM) in Tris-HCl buffer at pH 3 (a), 4 (b), 5 (c), 6 (d), 7 (e), 8 (f), 9 (g), 10 (h) and 11 (i) 100 mM at 37 °C.

Figure 9. Effects of pH(s) on the activity of choline oxidase from *Alcaligenes* species at 27 (▲) and 37 °C (■).

alkaline pH ranges with increasing pH, Trp fluorescence decreased. The overall decrease in emission intensity at higher pH values is accompanied by a slight overall red shift in the maximum. Such behavior suggests that, an enhanced exposure of the Trp residues to the aqueous solvent at very alkaline pH values took place. The results from extrinsic probe (Nile red) and intrinsic fluorescence are consistent with conformation changes resulting from changes in pH values.

The quenching experiments by acrylamide allowed reaching some information about conformational changes of choline oxidase by probing the solvent accessibility of fluorescent moieties. The initial linearity of Stern-Volmer plots does not distinguish between static and dynamic quenching (Figure 5). However, by rising the temperature from 27 to 37 °C, the K_{SV} at each pH increased significantly, thus fluorescence quenching of choline oxidase is pure collisional quenching. Fluorescence quenching data at various pH also show that the Trp residues are more exposed to the aqueous phase at pH 10 ($K_{SV} = 0.17$ and 0.33 at 27 and 37 °C, respectively) than at pH 8 ($K_{SV} = 0.07$ and 0.16 at 27 and 37 °C, respectively). This is consistent with the data from the intrinsic and Nile red fluorescence experiments. It is interesting to note that fluorescence quenching decreased rapidly at very alkaline pH(s) thus the significant increase in the solvent accessibility of Trp residues take place at these pH ranges.

CD has proved to be an ideal technique to monitor conformational changes in proteins, which can occur as a result of changes in experimental parameters such as pH, temperature, binding of ligands and so on.[50] Far-UV CD studies of choline oxidase at different pH values showed significant affected of pH on the secondary structure of the protein. The native protein has α-helical structure while at higher alkaline pHs a transition from α-helix to β-structure was appeared (Figure 6 and Tables 2 and 3) then, it can be concluded that at higher alkaline pH values, the β-sheet structure can induce in the secondary structure of choline oxidase. These results were confirmed with chemometric analysis. Transition from α-helix to β-structure appears to be physiologically important. It has been reported that the conformational switch from the α-helix to β-sheet leading to formation of amyloid structures.[51] In addition, the α-helix to β-sheet conformational transition(s) has been shown successfully in Alzheimer's AB peptide.[52] It is interesting to point out that at lower pH values the content of α-helix structure was increased (Figure 6 and Tables 2 and 3) and consequently prevent the access of the substrate (choline chloride) to the enzyme active site. Activity studies (Figure 9) showed that different pH values have an effect on the activity of choline oxidase. The main inactivation take place in the pH ranges 3-6 and 9-11, in which changes in the structure occurs leading to the enzyme inactivation. Taken together, the conclusion is reached that different pH values can bring about changes in enzyme structure, which in turn can affect choline oxidase interaction with the substrate (choline chloride), and its activity.

Results of thermal denaturation of protein at different pH by Far-UV-CD (Figure 7A and B) evaluated that choline oxidase has the most stability structure at pH 8 and the most instability occur at higher alkaline pH values. These results are consistent with conformation changes at higher alkaline pH values and transition from the α-helix to β-sheet structure.

Combining the results from extrinsic probe (Nile red), intrinsic fluorescence, acrylamide quenching, CD and chemometric analysis, we conclude that the structure of choline oxidase is modulated by the pH. The result obtaining from the present study probably provide useful information to design better biosensors for detection of choline, choline derivatives and organophosphorous compounds in biological and environmental samples. Also, for developing a curative agent that can specifically inhibit the formation of glycine betaine, and therefore render pathogens more susceptible to conventional treatment in the future.

References

1. Bhattacharyya, A. M.; Horowitz, P. *J. Biol. Chem.* **2000**, *275*, 14860.
2. Kettlun, A. M.; Espinosa, V.; Zanocco, A.; Valenzuela, M. A. *Braz. J. Med. Biol. Res.* **2000**, *33*, 725.
3. Qa'Dan, M.; Spyres, L. M.; Ballard, J. D. *Immun.* **2000**, *68*, 2470.
4. Hiratsuka, T. *J. Biol. Chem.* **1999**, *274*, 29156.
5. Ho, C.; Slater, S. J.; Stagliano, B. A.; Stubbs, C. D. *Biochem. J.* **1999**, *344*, 451.
6. Dixon, M.; Webb, E. C. *Enzymes*, 3rd ed.; Academic Press: New York, 1979; Chapter 4.
7. Bernheim, F.; Bernheim, M. L. C. *Am. J. Phsiol.* **1933**, *104*, 438.
8. Wells, I. C. *J. Biol. Chem.* **1954**, *207*, 575.
9. Williams, I. N.; Litwack, G. *J. Biol. Chem.* **1952**, *192*, 73.
10. Mann, P. J. G.; Woodward, H. E.; Quastel, J. H. *Biochem. J.* **1938**, *32*, 1024.
11. Ikuta, S.; Matuura, K.; Imamura, S.; Mistake, H.; Horiuti, Y. *J. Biochem.* **1977**, *82*, 157.
12. Yamada, H.; Mori, N.; Tani, Y. *Agric. Biol. Chem.* **1979**, *43*, 2173.
13. Ohta-Fukuyama, M.; Miyake, Y.; Emi, S.; Yamano, T. *J. Biochem.* **1980**, *88*, 197.
14. Ohta, M.; Miura, R.; Yamano, T.; Miyake, Y. *J Biochem.* (Tokyo) **1983**, *94*, 879.
15. Gadda, G. *Biochim. Biophys. Acta* **2003**, *1646*, 112.
16. Ohta-Fukuyama, M.; Miyake, Y.; Shiga, K. *J. Biochem.* **1980**, *88*, 205.
17. Gadda, G. *Biochim. Biophys. Acta* **2003**, *1650*, 4.
18. Cantor, C. H.; Schimmel, P. R. *Biophysical Chemistry*; W.H. Freeman and Company: New York, 1980.
19. Graham, J. E.; Wilkinson, B. J. *J. Bacteriol.* **1992**, *174*, 2711.
20. Bae, J. H.; Anderson, S. H.; Miller, K. *J. Appl. Environ. Microbiol.* **1993**, *59*, 2734.
21. Kaenjak, A.; Graham, J. E.; Wilkinson, B. J. *J. Bacteriol.* **1993**, *175*, 2400.
22. Culham, D. E.; Emmerson, K. S.; Lasby, B.; Mamelak, D.; Steer, B. A.; Gyles, C. L.; Villarejo, M.; Wood, J. M. *Can. J. Microbiol.* **1994**, *40*, 397.
23. Deshnium, P.; Gombos, Z.; Nishiyama, Y.; Murata, N. *J. Bacteriol.* **1997**, *179*, 339.
24. Deshnium, P.; Los, D. A.; Hayashi, H.; Mustardy, L.; Murata, N. *Plant. Mol. Biol.* **1995**, *29*, 897.
25. Alia; Hayashi, H.; Sakamoto, A.; Murata, N. *Plant J.* **1998**, *16*,

155.

26. Kempf, B.; Bremer, E. *Arch. Microbiol*. **1998**, *170*, 319.
27. Peddie, B. A.; Wong-She, J.; Randall, K.; Lever, M.; Chambers, S. T. *FEMS. Microbiol. Lett.* **1998**, *160*, 25.
28. Holmstrom, K. O.; Somersalo, S.; Mandal, A.; Palva, T. E.; Welin, B. *J. Exp. Bot.* **2000**, *51*, 177.
29. Sakamoto, A.; Alia; Murata, N. *Plant Mol. Biol*. **1998**, *38*, 1011.
30. Sakamoto, A.; Valverde, R.; Alia; Chen, T. H. H.; Murata, N. *Plant J.* **2000**, *22*, 449.
31. Tavakoli, H.; Ghourchian, H.; Moosavi-Movahedi, A. A.; Chilaka, F. C. *Int. J. Biol. Macromol.* **2005**, *36*, 318.
32. Guerrieri, A.; Monaci, L.; Quinto, M.; Palmisano, F. *Analyst* **2002**, *127*, 5.
33. Nunes, G. S.; Barcelo, D. *Analusis. Magazine* **1998**, *26*, 156.
34. Ajloo, D.; Behnam, H.; Saboury, A. A.; Mohamadi-Zonoz, F.; Ranjbar, B.; Moosavi-Movahedi, A. A.; Hasani, Z.; Alizadeh, K.; Gharanfoli, M.; Amani, M. *Bull. Korean Chem. Soc.* **2007**, *28*, 730.
35. Adams, M. J. *Chemometrics in Analytical Spectroscopy*, 2nd ed.; Royal Society of Chemistry: UK, 2004.
36. Diaz-Cruz, M. S.; Mendieta, J.; Tauler, R.; Esteban, M. *Anal. Chem*. **1999**, *71*, 4629.
37. Pirzadeh, P.; Moosavi-Movahedi, A. A.; Hemmateenejad, B.; Ahmad, F.; Shamsipur, M.; Saboury, A. A. *Colloids Surf. B: Biointerfaces* **2006**, *52*, 31.
38. Keesey, J. *Boehringer Mannheim Biochemicals*, 1st ed.; IN Biochemica Information: 1987; p 58.
39. Eftink, M. R.; Ghiron, C. A. *Anal. Biochem*. **1981**, *114*, 199.
40. Lehrer, S. S. *Biochemistry* **1971**, *10*, 3254.
41. Malinowski, E. R. *Factor Analysis in Chemistry*; Wiley & Sons: New York, 1991.
42. Ali, V.; Prakash, K.; Kulkarni, S.; Ahmad, A.; Madhusudan, K. P.; Bhakuni, V. *Biochemistry* **1999**, *38*, 13635.
43. Cardamone, M.; Puri, N. K. *Biochem. J.* **1992**, *282*, 589.
44. Kotik, M.; Zuber, H. *Eur. J. Biochem*. **1993**, *211*, 267.
45. Eftink, M. R.; Selvidge, L. A. *Biochemistry* **1982**, *21*, 117.
46. France, R. M.; Grossman, S. H. *Biochem. Biophys. Res. Commun*. **2000**, *296*, 709.
47. Sreerama, N.; Woody, R. W. *Protein Sci*. **2004**, *13*, 100.
48. Saboury, A. A.; Karbassi, F.; Haghbeen, K.; Ranjbar, B.; Moosavi-Movahedi, A. A.; Farzami, B. *Int. J. Biol. Macromol*. **2004**, *34*, 257.
49. Pace, C. N.; Shiley, B. A.; Thomson, J. A. *Protein Structure: A Practical Approach*; Creighton, T. E., Ed.; IRL Press: Oxford, 1990; p 311.
50. Kelly, S. M.; Price, N. C. *Curr. Prot. Pept. Sci*. **2000**, *1*, 349.
51. Bokvist, M.; Lindstrom, F.; Watts, A.; Grobner, G. *J. Mol. Biol*. **2004**, *335*, 1039.
52. Divsalar, A.; Saboury, A. A.; Mansoori-Torshizi, H.; Hemmatinejad, B. *Bull. Korean Chem. Soc.* **2006**, *27*, 1801.